



HAMAMATSU PRESENTS

ANALYTICAL TALKS

WATCH NOW 



Surface enhanced Raman spectroscopy-based evaluation of the membrane protein composition of the organohalide-respiring *Sulfurospirillum multivorans*

Dana Cialla-May^{1,2}  | Jennifer Gadkari³ | Andreea Winterfeld^{1,2} |
Uwe Hübner¹ | Karina Weber^{1,2} | Gabriele Diekert³ | Torsten Schubert³  |
Tobias Goris^{3,4} | Jürgen Popp^{1,2}

¹Leibniz Institute of Photonic Technology (IPHT) - Member of the research alliance "Leibniz Health Technologies", Albert-Einstein-Str. 9, Jena, 07745, Germany

²Institute of Physical Chemistry and Abbe Center of Photonics, Friedrich Schiller University Jena, Helmholtzweg 4, Jena, 07743, Germany

³Department of Applied and Ecological Microbiology, Institute of Microbiology, Friedrich Schiller University Jena, Philosophenweg 12, Jena, 07743, Germany

⁴Department of Molecular Toxicology, Group Intestinal Microbiology, German Institute of Human Nutrition, Potsdam-Rehbrücke Arthur-Scheunert-Allee, Nuthetal, 114-116 14558, Germany

Correspondence

Dana Cialla-May and Jürgen Popp,
Leibniz Institute of Photonic Technology
(IPHT), Albert-Einstein-Str. 9, Jena 07745,
Germany.
Email: dana.cialla-may@leibniz-ipht.de;
juergen.popp@leibniz-ipht.de

Present address

Tobias Goris, Intestinal Microbiology
Research Group, Department of
Molecular Toxicology, German Institute of
Human Nutrition, Potsdam-Rehbrücke,
Arthur-Scheunert-Allee 114-116,
Nuthetal, 14558, Germany.

Funding information

Bundesministerium für Bildung und
Forschung, Grant/Award Numbers:
01DN15028, 13N13856; Deutsches
Zentrum für Luft- und Raumfahrt, Grant/
Award Number: (DLR): 01DN15028;
Leibniz Research Cluster InfectoOptics,
Grant/Award Number: SAS-2015-HKI;
Strategy and Innovation Grant from the
Free State of Thuringia, Grant/Award
Number: 41-5507-2016; Deutsche
Forschungsgemeinschaft, Grant/Award
Number: FOR 1530

Abstract

Bacteria often employ different respiratory chains that comprise membrane proteins equipped with various cofactors. Monitoring the protein inventory that is present in the cells under a given cultivation condition is often difficult and time-consuming. One example of a metabolically versatile bacterium is the microaerophilic organohalide-respiring *Sulfurospirillum multivorans*. Here, we used surface enhanced Raman spectroscopy (SERS) to quickly identify the cofactors involved in the respiration of *S. multivorans*. We cultured the organism with either tetrachloroethene (perchloroethylene, PCE), fumarate, nitrate, or oxygen as electron acceptors. Because the corresponding terminal reductases of the four different respiratory chains harbor different cofactors, specific fingerprint signals in SERS were expected. Silver nanostructures fabricated by means of electron beam lithography were coated with the membrane fractions extracted from the four *S. multivorans* cultivations, and SERS spectra were recorded. In the case of *S. multivorans* cultivated with PCE, the recorded SERS spectra were dominated by Raman peaks specific for Vitamin B₁₂. This is attributed to the high abundance of the PCE reductive dehalogenase (PceA), the key enzyme in PCE respiration. After cultivation with oxygen, fumarate, or nitrate, no Raman spectral features of B₁₂ were found.

KEYWORDS

membrane proteins, perchloroethylene (PCE), silver nanostructures, surface enhanced Raman spectroscopy (SERS), Vitamin B₁₂

This is an open access article under the terms of the Creative Commons Attribution License, which permits use, distribution and reproduction in any medium, provided the original work is properly cited.

© 2020 The Authors. Journal of Raman Spectroscopy published by John Wiley & Sons Ltd

1 | INTRODUCTION

Sulfurospirillum multivorans, a representative of the free-living Campylobacterota (formerly Epsilonproteobacteria),^[1] is known to gain energy from tetrachloroethene (perchloroethylene, PCE) respiration.^[2] This type of anaerobic respiration is of environmental importance, because PCE represents a major groundwater contaminant. The key enzyme of PCE respiration is the PCE reductive dehalogenase, which is a membrane-bound terminal reductase that harbors a B₁₂ cofactor at the active site.^[3,4] The PCE reductive dehalogenase converts PCE via trichloroethene to *cis*-1,2-dichloroethene, which can be further dehalogenated by other bacteria in synthetic co-cultures or coupled anoxic–oxic bioreactors.^[5–9] *S. multivorans* was characterized as a metabolically flexible bacterium, able to use a high number of different electron donors and acceptors, including oxygen.^[10,11] Prolonged cultivation of *S. multivorans* with nitrate or fumarate instead of PCE as electron acceptor leads to the loss of the PCE respiratory chain components.^[12,13] Up to now, elaborate and time-consuming gene expression studies are needed to monitor the inventory of respiratory proteins present in the bacterium of interest. A rapid method to detect key enzymes of metabolic pathways, such as PceA, the PCE reductive dehalogenase, is highly desired. This would also be of advantage in the identification of potentially organohalide-respiring bacterial populations. The presence of cofactors in PceA and other metabolic key enzymes might prove beneficial for this detection, because they can often be rapidly identified spectroscopically. PceA for example harbors iron–sulfur clusters and adeninyl-norcobamide, a unique B₁₂ cofactor derivative.^[4,14,15] Other cofactors often found in respiratory enzymes are molybdopterin guanine dinucleotide in nitrate reductase or DMSO reductase,^[16–19] heme in cytochromes involved in, for example, oxygen respiration,^[20] or flavin components in fumarate respiration.^[21,22] The different protein composition of these terminal reductases in *S. multivorans* is depicted in Figure 1.

To evaluate the composition of membrane proteins of *S. multivorans* cultivated under different conditions, a specific, nondestructive and highly sensitive technique is required. Raman spectroscopy has proven to be a powerful tool in bioanalytics and imaging of biomaterials such as bacteria, cells, and tissue, because it allows for label-free and nondestructive recording of spectroscopic fingerprint information.^[23,24] As a consequence, all components within the cell or tissue sample are contributing to the overall Raman spectrum, and thus, complex spectral signatures are

obtained. To reduce the spectral complexity and to increase the sensitivity, surface enhanced Raman spectroscopy (SERS) was applied. SERS relies on the interaction of analyte molecules with plasmonic active nanostructured metal surfaces.^[25–27] Accordingly, only molecules in close proximity and with a high affinity toward the metallic surface will contribute to the overall SERS spectrum, and therefore, the complexity of the spectral fingerprint information is reduced. SERS is a powerful analytical tool in biophotonics, and its potential for the detection of biomolecules and biological samples, such as low molecular weight substances, DNA, and proteins, was illustrated previously.^[28,29] As an example to illustrate the capabilities of SERS in the investigation of the chemical composition of bacteria, the high throughput SERS detection of mycobacteria in a microfluidic environment was performed.^[30] First, the bacteria were homogenized, and second, after mixing the cell lysate with silver nanoparticles, SERS spectra were detected. Within that study, it was illustrated that the recorded SERS spectra are dominated by mycolic acid, solely present within the cell membrane of mycobacteria with a chemical structure specific for the different mycobacteria strains. Moreover, SERS was applied for the fast detection and quantification of low molecular weight substances produced in fermentation processes.^[31] Finally, SERS shows a high potential to be applied in environmental monitoring.^[32,33] Thus, SERS is an excellent candidate to investigate biological samples because it combines molecular specific information with a high sensitivity. Furthermore, the complexity of the spectral fingerprint information is reduced in comparison with Raman spectroscopy because only molecules with a high affinity toward the metallic surface will contribute to the overall SERS spectrum, making the method well suited for investigations in complex matrices.

In the present study, *S. multivorans* was cultivated with four different electron acceptors, PCE, fumarate, nitrate, as well as oxygen. To detect spectral fingerprint information with a high sensitivity, SERS spectroscopy was applied. Because of the different growth conditions, the recorded SERS spectra are dominated by various protein complexes present in the cytoplasmic membrane of the organism. In the case of PCE, the presence of the B₁₂ cofactor is expected, and the associated marker modes are identified under SERS conditions. This study demonstrates the potential of using SERS to detect low molecular weight substances produced by bacteria in fermentation processes or intoxication schemes based on the detection of specifically formed products such as protein complexes or other biochemical molecules.

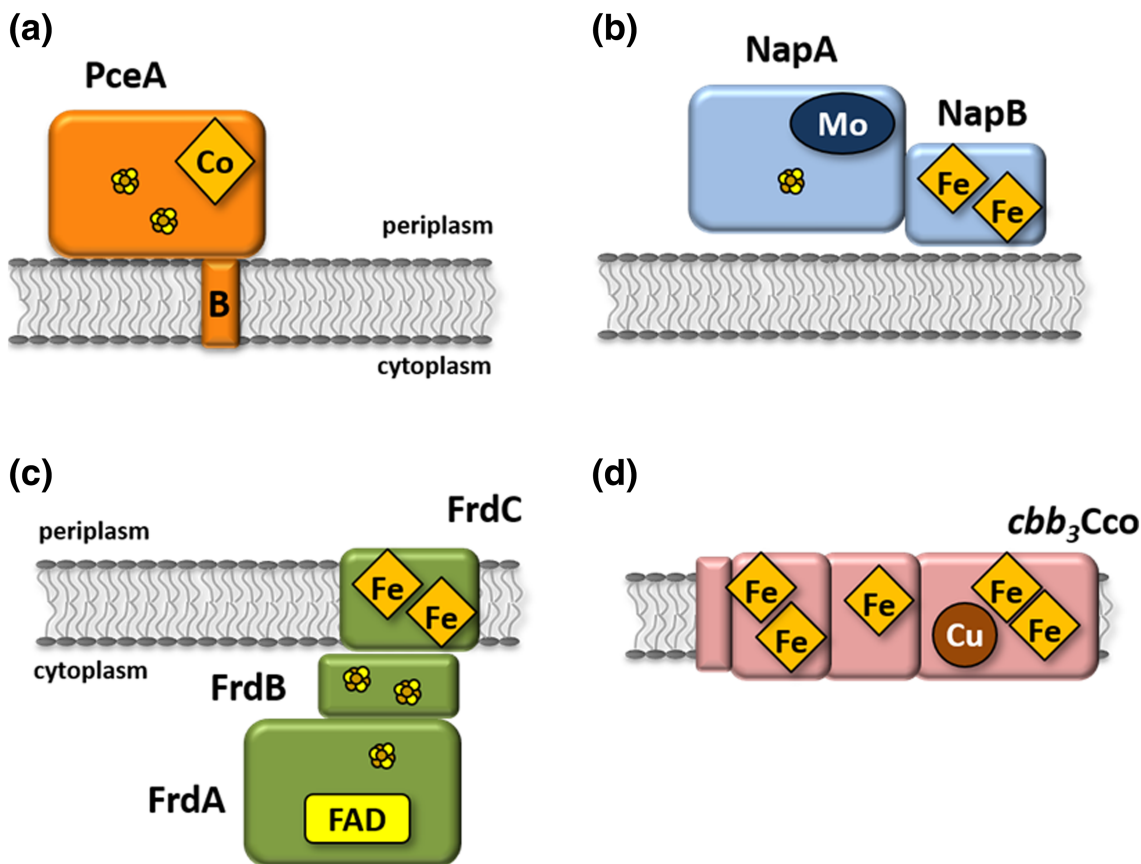


FIGURE 1 Schematic view on the protein and cofactor composition of the terminal reductases of *Sulfurospirillum multivorans*. (a) Perchloroethylene (PCE) reductive dehalogenase (PceA) harboring a B₁₂cofactor (Co) and cubane iron–sulfur clusters (as ball model). PceA is anchored to the membrane via the small anchor protein PceB. Note that PceAB might be part of a bigger complex with as yet uncharacterized iron–sulfur and/or heme proteins. (b) Periplasmic nitrate reductase (NapA) with a molybdopterin cofactor (Mo) and a cubane iron–sulfur cluster, NapB with heme cofactors (Fe). Note that NapAB might be part of a bigger complex with iron–sulfur and/or heme proteins. (c) Fumarate reductase (FrdA) with its flavin adenine dinucleotide (FAD) and cubane iron–sulfur cluster, its small electron-transferring subunit (FrdB) with two 4Fe-4S clusters, and the membrane-integral cytochrome (FrdC) with two heme groups. (d) The terminal oxidase cytochrome C oxidase Cco (*acbb3*-type oxidase as observed in Gadkari et al.^[11]), consisting of a catalytic subunit with a binuclear copper-heme center and three other subunits of which two are cytochromes containing heme groups

2 | MATERIAL AND METHODS

2.1 | Chemicals and reagents

Silver nitrate (ACS reagent, 99%), hydroxylamine hydrochloride (ReagentPlus, 99%), and sodium hydroxide have been purchased from Sigma-Aldrich. All chemicals used for the cultivation of *S. multivorans* were of the highest available purity and were purchased from Sigma-Aldrich. Gases were purchased from Linde.

2.2 | Cultivation of *S. multivorans*

In general, *S. multivorans* was cultivated as described previously.^[2,12] All cultivations were performed in 1-L anoxic medium in 2-L Schott bottles. Yeast extract was omitted from the medium; the cultivation was performed

under continuous shaking at 28°C. Pyruvate (40 mM) was used as electron donor under all conditions. PCE (10-mM nominal concentration) was added to the medium from a 0.5-M stock solution in hexadecane. Fumarate and nitrate concentrations were 40 mM each; oxygen (5% v/v) was supplied as gas into the nitrogen gas phase of gas-tight cultivation bottles. To generate cells devoid of PCE respiratory chain components, *S. multivorans* was cultivated for at least 60 transfers (10% inoculum each) in the presence of the desired electron acceptor (nitrate, fumarate, oxygen) without PCE.

2.3 | Preparation of the cell membranes

Cells were harvested at the late exponential growth phase via centrifugation (12,000×g, 10 min at 10°C) and then resuspended in 2 volumes Tris buffer (50-mM Tris-HCl,

pH 7.5) per weight wet cell mass. Disruption was performed in a French press (1,000 Psi corresponding to 6.9 MPa). For subcellular fractionation, the disrupted cells were centrifuged (260,000×g at 4°C for 45 min); the supernatant was discarded and the membranes were stored at −20°C for further use.

2.4 | Fabrication of SERS substrates

The SERS substrates, which contain 2D gratings with a period of 250 nm, were prepared by electron beam lithography, vacuum evaporation, and ion beam etching.^[34,35] A 4" fused silica wafer was cleaned by applying a peroxymonosulfuric acid solution, and subsequently, a thin undercoating (HMDS) and a 100-nm layer of the negative tone electron beam resist "maN2401" (micro resist technology GmbH) were prepared on the wafer by spin coating. As a next step, the resist was heated to 90°C for 180 s on a hotplate. In order to avoid charging effects, a 10-nm gold layer was evaporated on top of the electron beam resist. The application of the character projection-based electron beam technique^[35] of the shaped beam writer SB3500S (from Vistec Electron Beam GmbH) during the electron beam exposure, resulting in a changed resist solubility because of exposure, allowed for fast writing times (i.e., approximately 3 h for a 4" wafer). As a result, 140 chips (each chip has a size of $5 \times 10 \text{ mm}^2$) per wafer were fabricated. The chips were designed to comprise four SERS active gratings per chip with an individual size of $1 \times 1 \text{ mm}^2$. After the exposure, the gold layer was removed, and subsequently, the resist was developed in AZ MIF 726 developer for 30 s, and the wafer was finally rinsed with H₂O for 60 s. Thus, the soluble resist layer (nonexposed resist) was removed from the wafer surface. Further on, the structure was transferred into the fused silica surface by CHF₃-SF₆ inductively coupled plasma (ICP) etching employing a power of 300 W. Within our study, 2D gratings with a period of 250 nm and a etch depth of 100 nm were prepared. Finally, the residual resist layer was removed by means of oxygen plasma, and the wafer was cut in individual chips. To allow for comparable measuring conditions, the silver layer was freshly prepared by thermal evaporation at each measurement day employing high-purity (99.999%) silver granules as raw material. The thermal evaporation was performed using an oil-free background pressure in the lower 10^{-7} mbar range. The thickness of the silver layer was 40 nm, and the deposition rate was controlled via a quartz microbalance in situ. To allow for the control of each fabrication step, scanning electron microscopy (SEM) images were recorded by a JEOL JSM-6700F system.

Moreover, silver nanoparticles produced by the protocol published by Leopold and Lendl^[36] were applied. Here, silver nitrate (17 mg solved in 10-ml deionized water) was added to a mixture of hydroxylamine hydrochloride and sodium hydroxide (10.4 and 12 mg in 90-ml deionized water, respectively) under vigorous stirring. Instantaneously, a color change into gray-yellow is observed, and the stirring of the solution was continued for further 10 s. The colloidal silver nanoparticles were stored in solution at 4°C until the SERS measurements were conducted.

2.5 | Raman and SERS measurements

For all measurements, a commercial available Raman microscope (WITec alpha 300 SR, WITec GmbH, Ulm, Germany) was used. The Raman system was equipped with a 488-nm laser. The laser was focused on the sample employing a 100× microscope objective (NA 0.9), which is also employed to collect the Raman scattered light. The optical grating (600 g/mm) used allowed for recording the Raman and SERS spectra with a spectral resolution of $\sim 6 \text{ cm}^{-1}$.

To perform the Raman measurements, the membrane samples were transferred to a quartz microscope slide to avoid strong background Raman signals. For each cultivation condition, three replicates were investigated. For each replicate, 10 Raman spectra with an integration time of 2 s with five accumulations were recorded. The laser power used for the Raman experiments was 1.1 mW.

For the SERS measurements of the extracted purified B₁₂ cofactor (the extraction was performed according to the literature^[15]) of the PCE reductive dehalogenase from *S. multivorans*, the silver colloid (50 μl) was mixed with the aqueous solution of the analytes in a cuvette in a 1:1 ratio. The concentration of the B₁₂ compounds in the stock solutions was 1 μM. Prior to the analysis, 5 μl of a 1.2-N HCl solution and 5 μl of a 1-M KCl solution were added. For the measurements, the laser beam (power 18.5 mW) was focused into the solution. Every sample was analyzed in 10 Raman spectra with an integration time of 5 s.

To perform the SERS measurements of the cell membranes, the solid SERS substrates were applied, which showed a limit of detection of approximately 100 nM for the cofactor B₁₂ in a previous study.^[37] Here, the SERS substrate was coated by the sample, and the SERS spectra were recorded by using a laser power of 50 μW incident on the sample. We performed for each cell membrane sample (i.e., cultivation conditions) eight scans with $25 \times 25 \text{ μm}^2$ and 20×20 points (400 single spectra per

scan) with an integration time per point of 0.5 s. For each cultivation condition, three replicates were investigated. We estimated an average spectrum for each scan. In Table S1, we provided an assignment of the used SERS substrate for the investigation of the membrane samples.

Because of the absorption maximum of Vitamin B₁₂ around 550 nm,^[38] the applied excitation wavelength of 488 nm allows for an additional resonance Raman enhancement within the SERS experiments.

2.6 | Data analysis

All presented spectra have been analyzed using R (version 3.0.2)^[39] and plotted with Origin 8.5. For the data analysis, the spectra were background corrected using the sensitive nonlinear iterative peak (SNIP) algorithm^[40] and spike corrected using the Hampel filter.^[41]

3 | RESULTS AND DISCUSSION

The Raman spectra recorded for the isolated membrane fraction obtained from *S. multivorans* cells adapted to the four different growth conditions are shown in Figure 2. The Raman modes dominating the Raman spectra are marked. The band assignment was performed based on information from literature.^[42] Within the wavenumber region around 2,900 cm⁻¹, C—H stretching vibrations are found, that is, CH₃/CH₂ antisymmetric stretching at 2,927 cm⁻¹ as well as CH₃/CH₂ symmetric stretching at 2,875 cm⁻¹. Within the fingerprint region, the modes at 1,638, 1,573, and 1,367 cm⁻¹ are assigned to the Amide I, Amide II, and Amide III vibration, respectively. Finally, the Raman band at 1,445 cm⁻¹ is due to the CH₃/CH₂ antisymmetric bending vibration. All biomolecules present within the membrane fraction (mainly lipids and proteins) are contributing to the overall Raman spectra. As it is shown within Figure 2, the band ratio between the C—H stretching and the fingerprint region is varying, which might be due to changes in the lipid/protein content of the cell membranes for different growth conditions. Changes in the type of membrane proteins produced by *S. multivorans* have been monitored earlier by proteome and transcriptome analyses.^[12] Furthermore, the presence of PCE might cause an adaptation of the cell membrane composition as it has been observed earlier for nonhalogenated solvents.^[43] In Figure S1, the Raman spectra of the three batches are illustrated. However, because of the low signal to noise ratio, the Raman spectroscopic analysis does not allow for the identification of protein cofactors, which are expected to be higher concentrated in the cell membrane because of higher

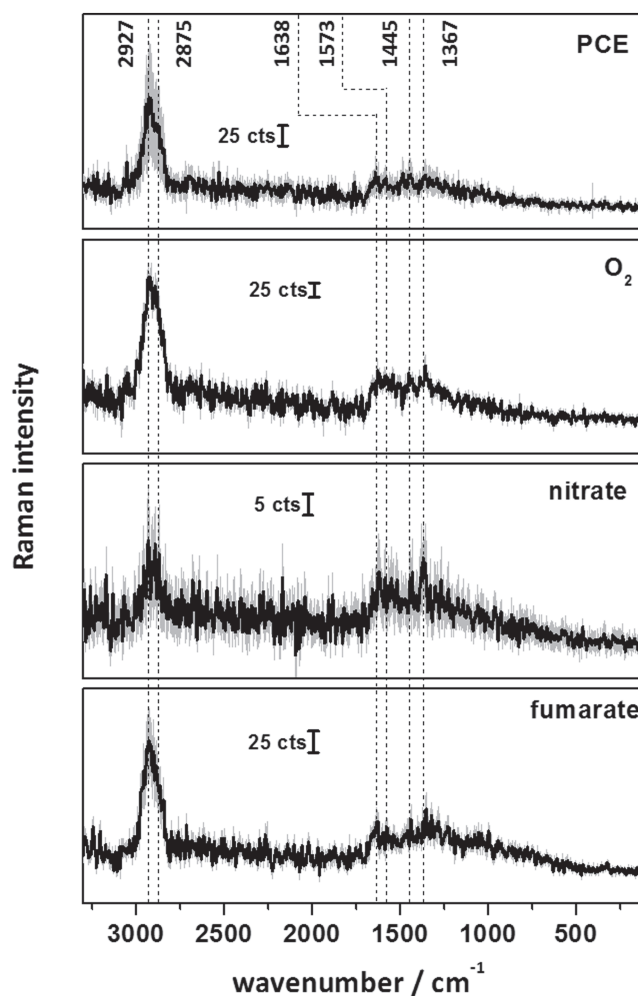


FIGURE 2 Raman spectra of *Sulfurospirillum multivorans* membranes extracted from cells cultivated with different electron acceptors (as depicted next to the spectra). The averaged spectra are denoted in black and the resulting standard deviation is denoted in gray (30 individual spectra from three batches). The spectral counts (cts) are given for each averaged spectrum

abundance of the respective terminal reductases in the different respiratory chains. Additionally, the background Raman spectrum of the quartz is provided in the supporting information to illustrate the specific Raman signature of the support material (Figure S2). No specific Raman signal of quartz is detected in the Raman spectra of the membranes.

In SERS, an intrinsic sample purification step is included when the analyte molecule of interest shows a higher affinity toward the metallic surface than the matrix molecules. Thus, the complexity of the spectral fingerprint information might be reduced when only view molecules or molecular classes are contributing to the SERS spectrum. Prior to the SERS investigations of the membranes, SERS analysis by using silver colloids of

different structural variants of the isolated B₁₂ cofactor was performed. As target analyte, the B₁₂ cofactor was chosen to illustrate the sensitivity of the SERS technique toward a B₁₂-containing enzyme. This in turn corresponds to the capacity of *S. multivorans* to dehalogenate PCE. In addition, we want to reveal the specificity of SERS to B₁₂/PCE reductive dehalogenase in comparison with other cultivation conditions. In Figure 3, the SERS spectra of various molecular structures of the B₁₂ cofactor are illustrated. The isolated B₁₂ structural variants differ in the type of lower base present in the nucleotide loop appendix of the tetrapyrrole ring (Figure 3a). All B₁₂ cofactors were purified from *S. multivorans*^[15] in the cyanofom that bears a cyano group as upper ligand to the cobalt and subsequently analyzed by SERS. As depicted in Figure 3b, SERS in comparison with Raman spectroscopy displayed a substantially higher sensitivity when a B₁₂ cofactor representative was tested. The spectral shape was very similar for all structural variants of the cofactor and a precursor molecule (cobinamide, Cbi) (Figure 3c). In comparison with published data, the same marker modes were detected.^[37,44,45] In detail, the marker mode at 1,593 cm⁻¹ represents a general feature

of vitamin B₁₂.^[37] The mode at 1,483 cm⁻¹ was assigned to an in-phase-stretching mode of the C=C bonds of the corrin ring.^[37] Moreover, the modes at 1,366 and 1,344 cm⁻¹ are due to an out-of-phase C—N and C—C stretching vibration as well as in-phase C—N stretching vibration.^[44] The corrin ring breathing mode was identified at 413 cm⁻¹.^[44] Taken together all the data, the SERS technique is well suited to detect the cofactor B₁₂. However, discrimination between structural variants was not possible without the application of sophisticated chemometric methods.

In the next step, we aimed at the spectral investigation of the isolated membranes of *S. multivorans* without further sample treatment. To avoid an incomplete coverage of the membranes when incubated with silver colloid and to allow for a direct and fast measurement, we applied regularly patterned silver arrays. In Figure 4, SEM images of the used SERS structures produced via electron beam lithography and silver deposition are depicted. The quartz template is coated with silver, forming highly uniformly distributed SERS active nanostructures (Figure 4a). Besides the silver layer on the bottom and on the top of the quartz nanosquares, the

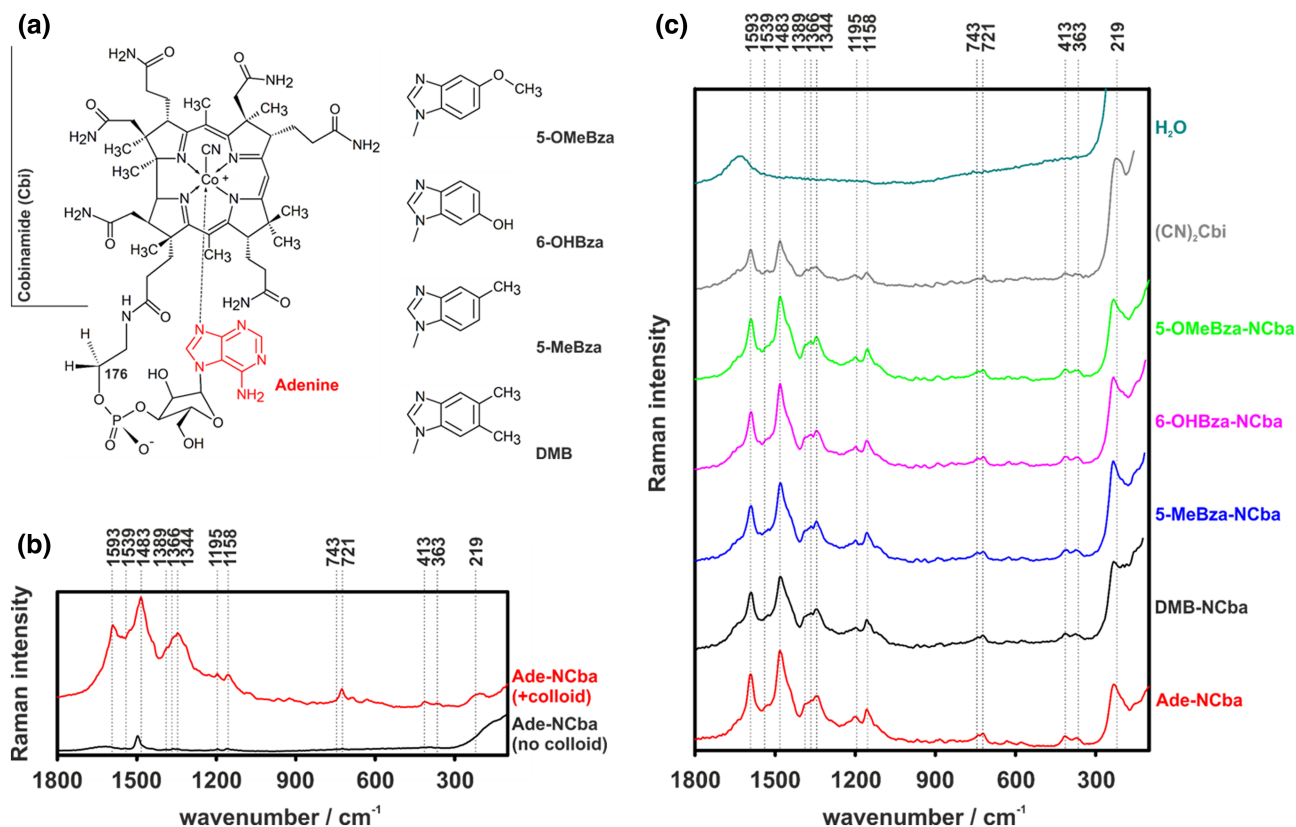


FIGURE 3 Surface enhanced Raman spectroscopy (SERS) analysis of the purified B₁₂ cofactor of the PCE reductive dehalogenase from *Sulfurospirillum multivorans*. (a) Structural variants used in this study. (b) Comparison of Raman spectroscopy and SERS. The purified adeninyl-norcobamide (Ade-NCba) was used as representative. (c) Normalized SERS spectra of different structural variants of the B₁₂ cofactor as well as the background signal by mixing the colloid with water

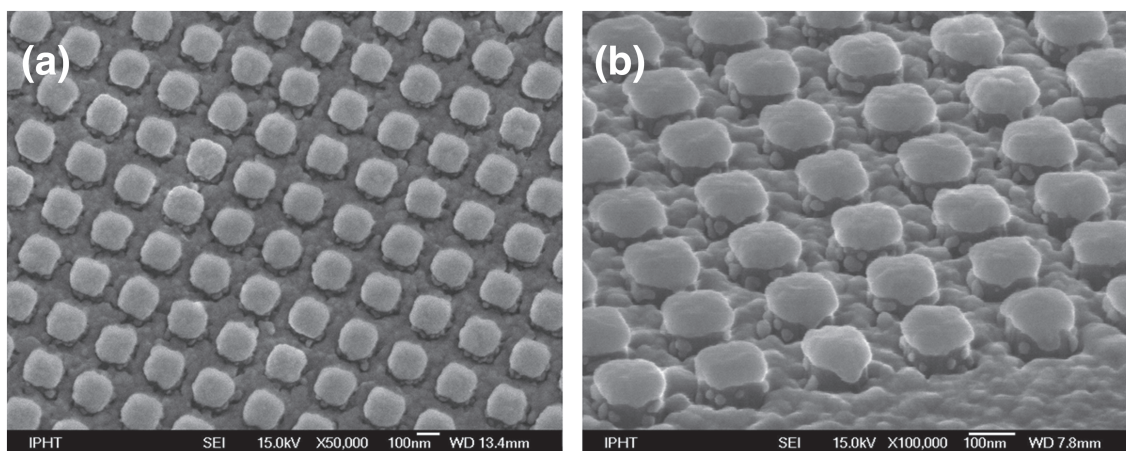


FIGURE 4 Scanning electron microscopy (SEM) images of the silver-coated quartz templates used as surface enhanced Raman spectroscopy (SERS) substrates: (a) illustration of the uniform arrangement and (b) detailed image showing nanoparticle arrangements on the steep edges of the template structure

steep edges are observed to be coated by silver nanoparticles (Figure 4b). For performing the SERS measurements, the SERS substrate was covered with a thin layer of the membrane fraction. Because of the viscosity of the bacterial membrane samples, the interaction of the membrane components with the metallic nanostructures is ensured during the SERS investigations.

The SERS spectra of the cell membranes obtained for the four different cultivation conditions are depicted in Figure 5. The standard deviation from the averaged SERS intensity values is illustrated by the light gray tube around the depicted mean value SERS spectrum. The background signal of the SERS substrates is illustrated in Figure S3. For all samples, a peak around $2,930\text{ cm}^{-1}$ was observed, which was attributed to C–H stretching vibrations as also found dominating within the Raman spectra.^[42] However, the CH stretching mode is not dominating the spectral fingerprint information by its intensity under SERS conditions, which is attributed to the fact that for Raman modes with high wavenumber shift, the influence of the second electromagnetic enhancement is decreased.^[46] Moreover, all samples showed a specific Raman marker mode around 230 cm^{-1} within the SERS spectra. This is a typically observed Raman mode under SERS conditions as it is due to the vibration between silver and nitrogen or oxygen.^[47,48] For all four different investigated cultivation conditions, each fingerprint region is specific for the changes within the cell membrane, which is attributed to the presence of different cofactors as illustrated in Figure 1.

In Figure 5a, the SERS spectra associated with the cultivation with PCE are illustrated, and the same marker modes as depicted in Figure 3 are found. The spectral profile and the spectral position of the

Raman modes are in good agreement with data from literature.^[37,44,45] Thus, we showed that the cofactor B_{12} is detectable directly within the cell membrane without further sample treatment steps. Obviously, the signal to noise ratio is highest in the case of PCE, which might be attributed to the additional resonance Raman enhancement of the cofactor B_{12} as the absorption maximum is around 550 nm .^[38] In Figure 5b, the SERS spectra of membranes obtained from cells cultivated with nitrate as electron are depicted. Under these conditions, the nitrate reductase, containing molybdopterin and heme, is produced. However, no specific marker modes of molybdopterin could be identified.^[49] The heme marker modes ν_2 , ν_3 , and ν_4 are located around $1,580$, $1,490$, and $1,360\text{ cm}^{-1}$ which could not be clearly assigned in our recorded SERS spectra.^[50] In Figure 5c, the SERS spectra of the cell membranes after cultivation with fumarate are illustrated. In the literature, marker modes of flavin adenine dinucleotide (FAD), the cofactor of the fumarate reductase, are identified at $1,486$, $1,395$, and $1,230\text{ cm}^{-1}$.^[51] At similar positions, we identified Raman modes in our spectra; however, because of the signal-to-noise ratio, a clear identification of FAD is impeded. Finally, in Figure 5d, the SERS spectra of membranes from cells cultivated in the presence of oxygen are depicted. Here, the bacterial membranes are expected to contain cytochrome C oxidase. However, no specific marker modes for cytochrome C oxidase^[52,53] could be identified, which is due to the low signal-to-noise ratio of the recorded SERS spectra.

These investigations demonstrated that we are able to identify when cells were cultivated in the presence of PCE by means of the sensitive and molecular specific detection of B_{12} via SERS. The detection of other

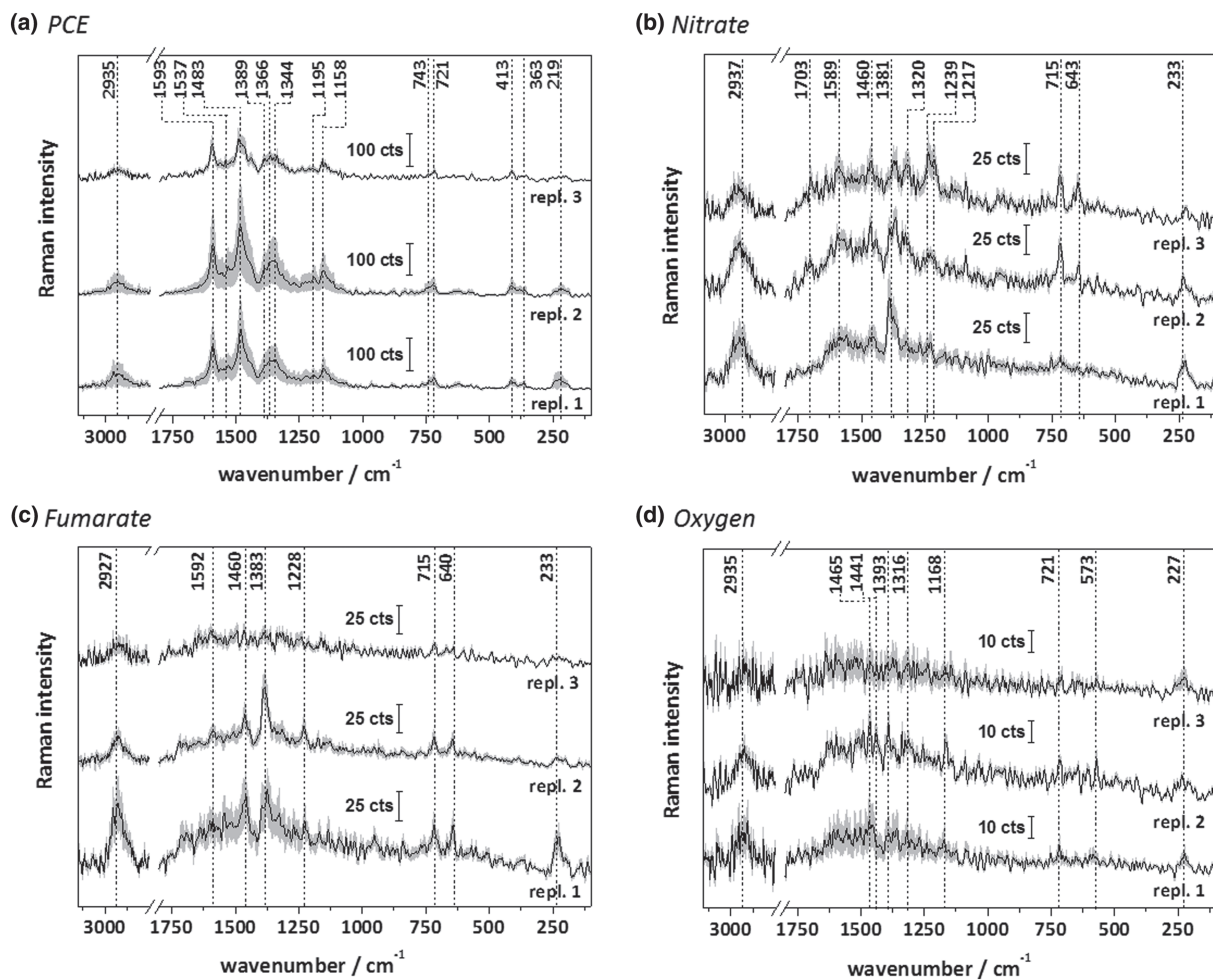


FIGURE 5 Surface enhanced Raman spectroscopy (SERS) analysis of the cell membrane of *Sulfurospirillum multivorans* by using regularly patterned SERS substrates for four different cultivation conditions: (a) perchloroethylene (PCE), (b) nitrate, (c) fumarate, and (d) oxygen

cofactors than B₁₂ was not feasible in our study because of the low signal-to-noise ratios of the corresponding SERS spectra, which might be associated with the less unique cofactor in the case of nitrate reductase, fumarate reductase, and cytochrome C oxidase: *S. multivorans* is equipped with several putative molybdopterin-containing enzymes,^[10] of which some are constitutively produced and present in membranes.^[12] A similar situation can be attributed to the other cofactors present in the respiratory chains such as FAD and heme, which are common to several enzymes. Opposed to this, PCE-cultivated *S. multivorans* cells harbor exclusively the PCE dehalogenase as a B₁₂-containing enzyme under the given conditions.^[12] Possibly, the detection of molybdopterin-containing enzymes would be possible in bacteria that produce high amounts of only one enzyme containing this cofactor. Our proposed SERS-sensing method would be suitable to identify the detoxification of PCE in bioreactors simply by monitoring the cofactors

produced in the bacterial membrane. When PCE is present, PCE reductive dehalogenases containing B₁₂ are produced, which can be detected by SERS spectroscopy.

Finally, the potential of the SERS technique for a rapid assessment of the capacity of PCE detoxification in reactors by the usage of *S. multivorans* is illustrated in Figure 6. Here, *S. multivorans* cells, cultivated with PCE, were transferred to the SERS active surface, and the same marker modes of the cofactor B₁₂ were identified as already found in the SERS spectra of the extracted cofactor B₁₂, Ade-NCba (see also Figure 3), and the cell membranes upon cultivation in the presence of PCE (see also Figure 5a). Even after omitting the extraction of the cell membrane, the SERS spectra showed a good signal-to-noise ratio. As a consequence, our applied SERS detection scheme is suited to monitor the detoxification process of PCE within reactors simply by proving the production of the cofactor B₁₂ in *S. multivorans* cells.

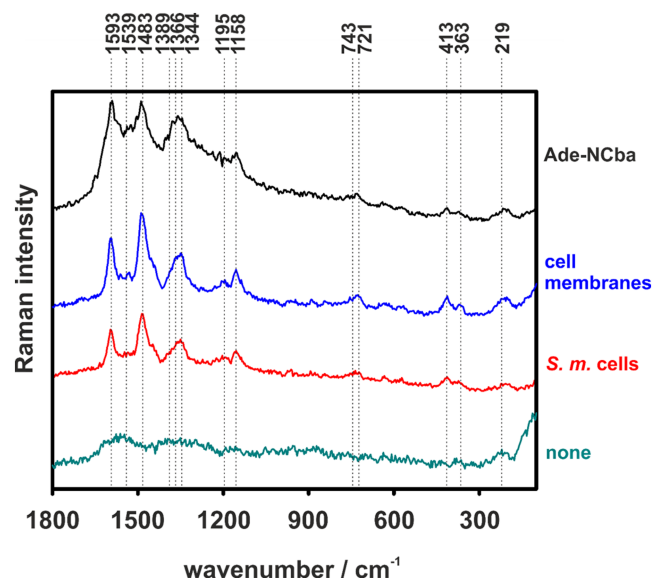


FIGURE 6 Surface enhanced Raman spectroscopy (SERS) analysis of *Sulfurospirillum multivorans* cells transferred on regularly patterned SERS substrates in comparison with the SERS spectrum of cell membranes as well as the isolated B₁₂cofactor (Ade-NCba). The blank spectrum is labeled with “none.” The spectra were normalized

4 | CONCLUSION

Taken together, we showed an easy, rapid, and nondestructive method to detect a B₁₂-containing enzyme of the respiratory chain in bacterial membranes by means of SERS. The specific detection of the PCE reductive dehalogenase can facilitate the detection of active bacterial dehalogenation processes that proceed in low-oxygen environments. In the future, this technique also might aid in other processes where the rapid detection of B₁₂-containing enzymes might be of advantage, which are not contained in membranes. Although here we failed to detect the enzymes containing other cofactors than B₁₂, it might be possible to detect these with refined methods, in other organisms or with other enzymes containing SERS-responsive cofactors such as other tetrapyrroles or metal clusters.

ACKNOWLEDGEMENT

J. Gadkari, T. Schubert, T. Goris, and G. Diekert would like to gratefully acknowledge the DFG funding for the research unit FOR 1530. The work of T Schubert was financially supported by a Strategy and Innovation Grant from the Free State of Thuringia (41-5507-2016) and the Leibniz Research Cluster InfectoOptics (SAS-2015-HKI). Funding of the research project “|EXASENS” (13N13856) by the Federal Ministry of Education and Research (BMBF), Germany is gratefully acknowledged. The

project “MycoNET²” (01DN15028) is funded by BMBF and German Aerospace Center (DLR).

ORCID

Dana Cialla-May  <https://orcid.org/0000-0002-8577-1490>

Torsten Schubert  <https://orcid.org/0000-0002-6569-1194>

REFERENCES

- [1] D. W. Waite, M. S. Chuvochina, P. Hugenholtz, in *Bergey's Manual of Systematics of Archaea and Bacteria*, (Eds: W. B. Whitman, F. Rainey, P. Kämpfer, M. Trujillo, J. Chun, P. DeVos, B. Hedlund, S. Dedysh), John Wiley & Sons, Inc **2019** 1.
- [2] H. Scholz-Muramatsu, A. Neumann, M. Meßmer, E. Moore, G. Diekert, *Arch. Microbiol.* **1995**, *163*, 48.
- [3] A. Neumann, G. Wohlfarth, G. Diekert, *J. Biol. Chem.* **1996**, *271*, 16515.
- [4] M. Bommer, C. Kunze, J. Fessler, T. Schubert, G. Diekert, H. Dobbek, *Science* **2014**, *346*, 455.
- [5] P.-G. Rieger, H.-M. Meier, M. Gerle, U. Vogt, T. Groth, H.-J. Knackmuss, *J. Biotechnol.* **2002**, *94*, 101.
- [6] M. Eisenbeis, P. Bauer-Kreisel, H. Scholz-Muramatsu, *Water Sci. Technol.* **1997**, *36*, 191.
- [7] C. Hörber, N. Christiansen, E. Arvin, B. K. Ahring, *Appl. Environ. Microbiol.* **1998**, *64*, 1860.
- [8] C. Hörber, N. Christensen, E. Arvin, B. Kiær Ahring, *Appl. Microbiol. Biotechnol.* **1999**, *51*, 694.
- [9] S. Kruse, D. Türkowsky, J. Birkigt, B. Matturro, S. Franke, N. Jehmlich, M. V. Bergen, M. Westermann, S. Rossetti, I. Nijenhuis, L. Adrian, G. Diekert, T. Goris, *bioRxiv* **2019**, 526210.
- [10] T. Goris, T. Schubert, J. Gadkari, T. Wubet, M. Tarkka, F. Buscot, L. Adrian, G. Diekert, *Environ. Microbiol.* **2014**, *16*, 3562.
- [11] J. Gadkari, T. Goris, C. L. Schiffmann, R. Rubick, L. Adrian, T. Schubert, G. Diekert, *FEMS Microbiol. Ecol.* **2018**, *94*.
- [12] T. Goris, C. L. Schiffmann, J. Gadkari, T. Schubert, J. Seifert, N. Jehmlich, M. von Bergen, G. Diekert, *Sci. Rep.* **2015**, *5*, 13794.
- [13] M. John, R. Rubick, R. P. H. Schmitz, J. Rakoczy, T. Schubert, G. Diekert, *J. Bacteriol.* **2009**, *191*, 1650.
- [14] B. Krätler, W. Fieber, S. Ostermann, M. Fasching, K.-H. Ongania, K. Gruber, C. Kratky, C. Mikl, A. Siebert, G. Diekert, *Helv. Chim. Acta* **2003**, *86*, 3698.
- [15] S. Keller, C. Kunze, M. Bommer, C. Paetz, R. C. Menezes, A. Svatoš, H. Dobbek, T. Schubert, *J. Bacteriol.* **2018**, *200*, e00584.
- [16] R. A. Rothery, G. J. Workun, J. H. Weiner, *Biochim. Biophys. Acta, Biomembr.* **2008**, *1778*, 1897.
- [17] J. L. Johnson, N. R. Bastian, K. V. Rajagopalan, *Proc. Natl. Acad. Sci. U. S. A.* **1990**, *87*, 3190.
- [18] K. Frunzke, B. Heiss, O. Meyer, W. G. Zumft, *FEMS Microbiol. Lett.* **1993**, *113*, 241.
- [19] S. Leimkühler, C. Iobbi-Nivol, *FEMS Microbiol. Rev.* **2016**, *40*, 1.
- [20] V. Borisov, M. Verkhovsky, *EcoSal Plus* **2015**, *6*.
- [21] C. R. D. Lancaster, A. Kröger, M. Auer, H. Michel, *Nature* **1999**, *402*, 377.

- [22] C. Lancaster, A. Kröger, *Biochim. Biophys. Acta, Bioenerg.* **2000**, 1459, 422.
- [23] C. Krafft, M. Schmitt, I. W. Schie, D. Cialla-May, C. Matthäus, T. Bocklitz, J. Popp, *Angew. Chem., Int. Ed.* **2017**, 56, 4392.
- [24] A. N. Kuzmin, A. Pliss, P. N. Prasad, *Biosensors* **2017**, 7, 52.
- [25] M. F. Cardinal, E. Vander Ende, R. A. Hackler, M. O. McAnally, P. C. Stair, G. C. Schatz, R. P. van Duyne, *Chem. Soc. Rev.* **2017**, 46, 3886.
- [26] D. Cialla-May, X. S. Zheng, K. Weber, J. Popp, *Chem. Soc. Rev.* **2017**, 46, 3945.
- [27] X.-S. Zheng, I. J. Jahn, K. Weber, D. Cialla-May, J. Popp, *Spectrochim. Acta Part A* **2018**, 197, 56.
- [28] M. Kahraman, E. R. Mullen, A. Korkmaz, S. Wachsmann-Hogiu, *Nano* **2017**, 6, 831.
- [29] D. Cialla, S. Pollok, C. Steinbrücker, K. Weber, J. Popp, *Nano* **2014**, 3, 383.
- [30] A. Mühligh, T. Bocklitz, I. Labugger, S. Dees, S. Henk, E. Richter, S. Andres, M. Merker, S. Stöckel, K. Weber, D. Cialla-May, J. Popp, *Anal. Chem.* **2016**, 88, 7998.
- [31] H. Ren, Z. Chen, X. Zhang, Y. Zhao, Z. Wang, Z. Wu, H. Xu, *J. Anal. Methods Chem.* **2016**, 2016, 4910630.
- [32] H. Takei, J. Saito, K. Kato, H. Vieker, A. Beyer, A. Götzhäuser, *J. Nanomater.* **2015**, 2015, 316189.
- [33] S. Patze, U. Huebner, F. Liebold, K. Weber, D. Cialla-May, J. Popp, *Anal. Chim. Acta* **2017**, 949, 1.
- [34] U. Huebner, K. Weber, D. Cialla, H. Schneidewind, M. Zeisberger, H. G. Meyer, J. Popp, *Microelectron. Eng.* **2011**, 88, 1761.
- [35] U. Huebner, M. Falkner, U. Zeitner, M. Banasch, K. Dietrich, E.-B. Kley, *Proc. SPIE* **2014**, 9231, 92310E.
- [36] N. Leopold, B. Lendl, *J. Phys. Chem. B* **2003**, 107, 5723.
- [37] A. I. Radu, M. Kuellmer, B. Giese, U. Huebner, K. Weber, D. Cialla-May, J. Popp, *Talanta* **2016**, 160, 289.
- [38] J. Wang, J. Wei, S. Su, J. Qiu, *New J. Chem.* **2015**, 39, 501.
- [39] R Core Team. Vienna, Austria. Available online at <https://www.R-project.org/>. **2018**.
- [40] M. Omer, H. Negm, R. Kinjo, Y.-W. Choi, K. Yoshida, T. Konstantin, M. Shibata, K. Shimahashi, H. Imon, H. Zen, T. Hori, T. Kii, K. Masuda, H. Ohgaki, in *Zero-Carbon Energy Kyoto 2012*, (Ed: T. Yao), Springer, Tokyo **2013** 245.
- [41] A. Quintero Rincón, M. Risk, S. Liberczu, *ARGENCON 2012 – IEEE Latin American Transactions – Córdoba, Argentina, 13 al 15 de Junio de 2012* **2012**, 89.
- [42] C. Matthäus, B. Bird, M. Miljković, T. Chernenko, M. Romeo, M. Diem, *Methods Cell Biol.* **2008**, 89, 275.
- [43] J. L. Ramos, E. Duque, M.-T. Gallegos, P. Godoy, M. I. Ramos-González, A. Rojas, A. Wilson Terán, A. Segura, *Annu. Rev. Microbiol.* **2002**, 56, 743.
- [44] T. Andruniow, M. Z. Zgierski, P. M. Kozlowski, *J. Phys. Chem. A* **2002**, 106, 1365.
- [45] S. Dong, R. Padmakumar, R. Banerjee, T. G. Spiro, *Inorg. Chim. Acta* **1998**, 270, 392.
- [46] D. Cialla, J. Petschulat, U. Hübner, H. Schneidewind, M. Zeisberger, R. Mattheis, T. Pertsch, M. Schmitt, R. Möller, J. Popp, *ChemPhysChem* **2010**, 11, 1918.
- [47] J. Chowdhury, K. M. Mukherjee, T. N. Misra, *J. Raman Spectrosc.* **2000**, 31, 427.
- [48] O. Žukovskaja, I. J. Jahn, K. Weber, D. Cialla-May, J. Popp, *Sensors* **2017**, 17, 1704.
- [49] L. Kilpatrick, K. V. Rajagopalan, J. Hilton, N. R. Bastian, E. I. Stiefel, R. S. Pilato, T. G. Spiro, *Biochemistry* **1995**, 34, 3032.
- [50] E. L. Green, S. Taoka, R. Banerjee, T. M. Loehr, *Biochemistry* **2001**, 40, 459.
- [51] D. Sun, G. Qi, F. Cao, W. Xu, Q. Chen, S. Xu, *Talanta* **2017**, 171, 159.
- [52] M. Sezer, P. Kielb, U. Kuhlmann, H. Mohrmann, C. Schulz, D. Heinrich, R. Schlesinger, J. Heberle, I. M. Weidinger, *J. Phys. Chem. B* **2015**, 119, 9586.
- [53] M. Sezer, A.-L. Woelke, E. W. Knapp, R. Schlesinger, M. A. Mroginski, I. M. Weidinger, *Biochim. Biophys. Acta, Bioenerg.* **2017**, 1858, 103.

SUPPORTING INFORMATION

Additional supporting information may be found online in the Supporting Information section at the end of this article.

How to cite this article: Cialla-May D, Gadkari J, Winterfeld A, et al. Surface enhanced Raman spectroscopy-based evaluation of the membrane protein composition of the organohalide-respiring *Sulfurospirillum multivorans*. *J Raman Spectrosc.* 2021;52:458–467. <https://doi.org/10.1002/jrs.6029>